Journal of Alloys and Compounds 504S (2010) S226–S229

Contents lists available at ScienceDirect

Journal of Alloys and Compounds

journal homepage: www.elsevier.com/locate/jallcom

# Evaluation of the crystal volume fraction in a partially nanocrystallized bulk metallic glass

S. Gravier*, P. Donnadieu, S. Lay, B. Doisneau, F. Bley, L. Salvo, J.J. Blandin

*SIMAP laboratory, Grenoble University/CNRS/UJF/Grenoble-INP, BP 46, 38042 Saint-Martin d'Hères, France*

ARTICLE INFO

*Article history:*
Received 21 July 2009
Received in revised form 3 May 2010
Accepted 4 May 2010
Available online 9 May 2010

*Keywords:*
Metallic glasses
Crystallization
Microstructure
Volume fraction
X-ray diffraction

ABSTRACT

Bulk metallic glasses are out of equilibrium materials and consequently they tend to crystallize when heated in the supercooled liquid region. Crystallization has been shown to change drastically the properties of the BMG. However, in order to quantify these changes due to crystallization, it is first necessary to get detailed information about the structure evolution and especially the size and volume fraction of the crystallites. Partial crystallization of the Vitreloy 1 metallic glass is carried out in the supercooled liquid region. The crystallization is quantified by DSC and XRD measurements and the obtained values are compared. An important difference is observed and the maximum volume fraction is compared to the value predicted by appropriate numerical simulations. It is shown that XRD measurements seem to be appropriate to calculate the crystallite volume fraction while care must be taken if using DSC measurements.



## 1. Introduction

Bulk metallic glasses (BMG) are very attractive materials since they exhibit not only unique mechanical properties at room temperature, such as high strength and large elastic limit [1] but also a very large ductility when they are deformed in the viscous state (i.e. at high temperatures above $0.7T_g$, with $T_g$ the glass transition temperature of the glass) [2–4]. In this regime, due to high plastic stability, components with very complex shapes can be produced. In consequence, BMGs are considered as interesting structural materials in the field of near net shape fabrication of structural components. However, resulting from their way of elaboration, BMGs are materials with a microstructure which is out of equilibrium. In consequence, when they are maintained at high temperature, crystallization is expected to occur. Such crystallization, even if it is partial, generally affects the mechanical properties at room temperature but also the viscous flow at high temperature. At room temperature, the fracture stress measured in compression generally increases up to a critical crystal content and then drops drastically [1,5–7], this change being also generally related to a change in the fracture mechanisms. The effect of nanocrystallization on high temperature deformation remains quite poorly documented, but frequently, after an incubation time, the viscosity increases sharply [8–16].

The ability to use mechanical models (i.e. for instance mechanical models of dispersed hard particles in a viscous matrix) to predict such effect of nanocrystallization on the mechanical response of a metallic glass requires to get reliable information about the crystal volume fraction $f_v$. The most frequently used way to estimate $f_v$ is based on data from differential scanning calorimetry (DSC) [13,14,17] according to:

$$f_v = \int_0^t H(t)\,dt \Big/ \int_0^\infty H(t)\,dt \quad (1)$$

where $H(t)$ is the released heat flux. This equation assumes strong hypothesis like for example that the enthalpy of crystallization does not vary with the degree of crystallization, or that one kind of crystal dominates the crystallization process. It also assumes that the alloy is fully crystallized at the end of the studied transformation. Other non-direct techniques can also be used like density or resistivity measurements but they need to know associated characteristics of the crystalline phases, which are generally unknown [18]. Very few studies have been carried out to measure directly the crystal volume fraction in partially crystallized metallic glasses except one attempt carried out by Wesseling et al. [19] who concluded that there could have some differences between the various measurements methods but who did not discriminate between them. The authors also concluded that direct measurements through bright field TEM observations were hard to achieve due to the rapid superposition of crystallites in the analyzed thickness.

* Corresponding author. Tel.: +33 476826379.
*E-mail address:* sebastien.gravier@simap.grenoble-inp.fr (S. Gravier).

0925-8388/$ – see front matter © 2010 Elsevier B.V. All rights reserved.
doi:10.1016/j.jallcom.2010.05.008

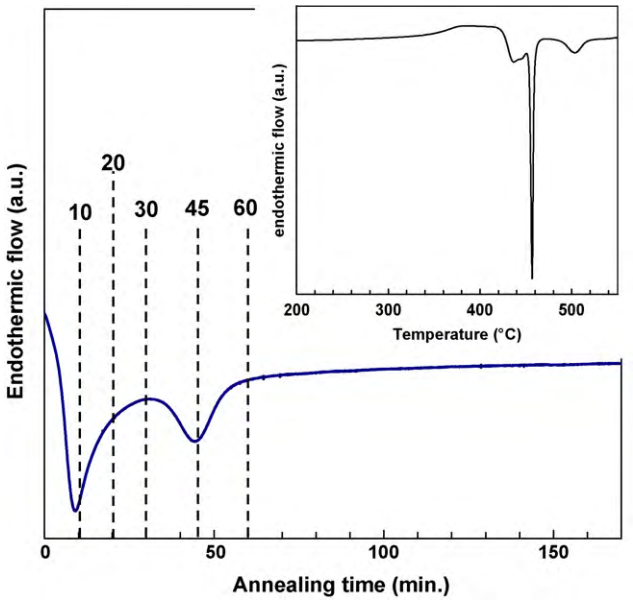


**Fig. 1.** Isothermal DSC curve at 410 °C where selected annealing time are pointed out. The insert displays a DSC scanning curve of the amorphous alloy at 10 °C/min.

In the present paper, we report XRD measurements of volume fraction on a partially crystallized zirconium based BMG. Those measurements are compared to what is measured by DSC heat release measurements. Information concerning the shape and the size distributions of the crystals in the residual amorphous matrix are deduced from TEM observations of the partially crystallized alloys. Starting from these data, a numerical simulation is carried out, predicting the critical volume fraction of non-intersecting particles which can be dispersed in a given medium. This critical volume fraction is discussed in relation to the measurements.

## 2. Experimental

The investigated alloy was supplied by Howmet Corp. (USA). Differential scanning calorimetry was performed in a Perkin Elmer diamond DSC. X-Ray Diffraction (XRD) with Cu Kα radiation was used to investigate the microstructure evolution after annealing. Transmission electron microscopy (TEM) was also carried out, the observations being performed at 300 kV in a JEOL 3010 microscope. An ion beam milling method was used to prepare the thin foils.

## 3. Results and discussions

The studied alloy is the Vit1 BMG ($Zr_{41.2}Ti_{13.8}Cu_{12.5}Ni_{10}Be_{22.5}$, at.%), which has been widely studied in the past [20–22]. Despite the large number of studies, the detailed mechanisms of crystallization in this glass remain under debate. DSC curves obtained in continuous heating conditions generally display three successive crystallization peaks (see insert in Fig. 1) and after the last one, nearly complete crystallization is achieved since a lot of grain boundaries between the crystals can be observed by TEM [6]. The total energy release corresponding to those three exothermic peaks is 79 J/g and thus corresponds to the maximum volume fraction attainable of around 100%. When the alloy is heated and maintained at 410 °C in the supercooled liquid region, crystallization ends roughly after 60 min as illustrated by the isothermal DSC curve shown in Fig. 1. In this figure, two peaks can be observed that correspond to the first two crystallization events [6]. Finally, after approximately 60 min, the heat flux appears stabilized and the driving force is no longer high enough to continue the crystallization. We can hence calculate the value of the crystallite volume fraction as a function of annealing time using Eq. (1). The released heat flux for the various annealing times can be calculated through the result of Fig. 1 and the total heat release corresponding to the complete crystallization is calculated to be 79 J/g. Volume fraction for the highlighted holding times in Fig. 1 (10, 20, 30, 45 and 60 min) are given in Table 1.

**Table 1**
Variation of the crystal volume fraction as a function of the annealing time at 410 °C using DSC and XRD measurements.

| $t$ (min) | 10 | 20 | 30 | 45 | 60 |
|---|---|---|---|---|---|
| $f_v$ by DSC | 0.10 | 0.38 | 0.50 | 0.68 | 0.84 |
| $f_v$ by XRD | 0.07 | 0.17 | 0.27 | 0.32 | 0.45 |

Some direct information can be obtained from XRD measurements [19]. Indeed, in the present case, the nanocomposite can be roughly described as an amorphous matrix with a random distribution of crystallites. Since the particles take any orientation in space and since they have no orientation relationship with the matrix or between each other, they are spatially incoherent with respect to the matrix and with respect to each other. Hence, as in a gas or in a non-textured polycrystal, the total diffraction intensity $I_t(q)$ can be considered as the sum of the diffraction intensities of the amorphous matrix $I_a$ and the crystallites $I_c$ [23,24]:

$$I_t(q) = I_a(q) + I_c(q) \quad (2)$$

Under the assumption of a narrow enough size distribution of crystallites characterized by similar average diffusion factor, $I_c(q)$ is proportional to the number of atoms in all the crystallites within the diffracting volume. After integration of the intensity over the reciprocal space, it can be shown that the contribution of each phase is thus proportional to its volume fraction. In such a framework, it becomes straightforward using the XRD patterns to separate each contribution. The volume fraction will be given by the ratio of the integrated intensity corresponding to each contribution. It is worth noting that the link between volume fraction and integrated intensity is made under several assumptions: (*i*) a narrow particle size distribution; (*ii*) a limited variation of density between amorphous and crystallized states. In the present case, the density of amorphous state compared to the corresponding crystal, varies only by about 1% [25].

Fig. 2 shows a typical example of this procedure in the case of the alloy annealed for 60 min at 410 °C. The shape of the curve

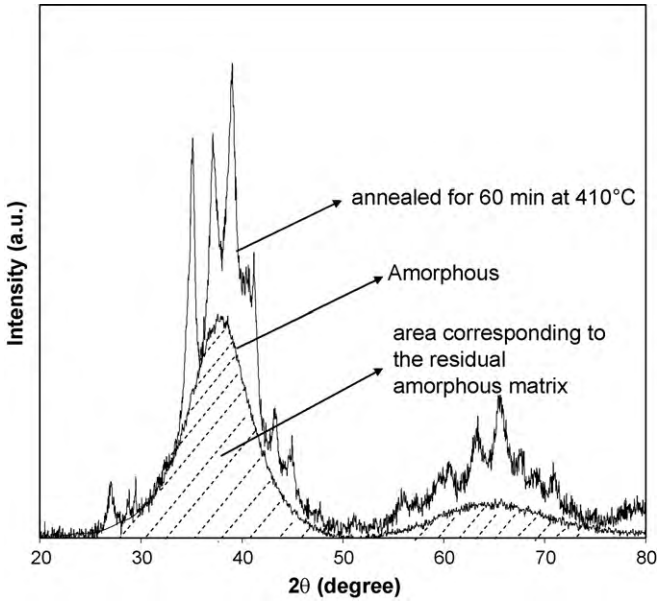


**Fig. 2.** XRD spectra for the amorphous alloy and the specimen annealed for 60 min at 410 °C and a representation of the calculation of the crystalline volume fraction.

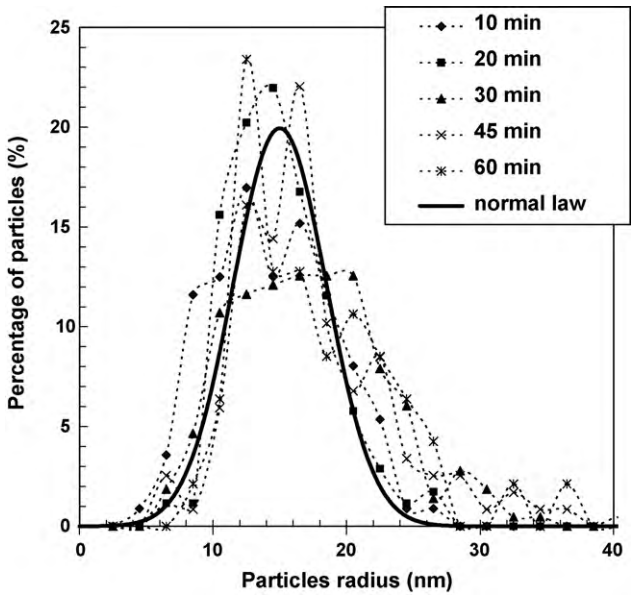


**Fig. 3.** Distribution of the particles radius measured by TEM depending on the annealing time at 410 °C. The selected normal law corresponding to Eq. (3) is also plotted.

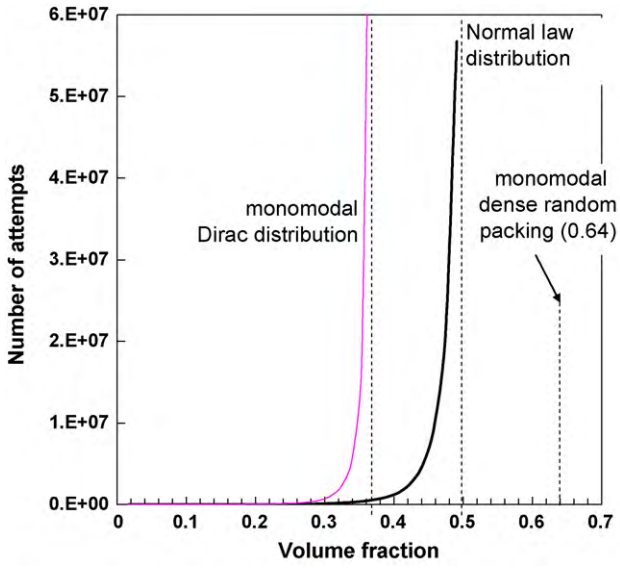


**Fig. 4.** Numerical simulations results calculating the maximum volume fraction attainable for two particles distributions; a monomodal Dirac distribution and the normal law distribution with the parameters defined in Eq. (3). The value corresponding to monomodal dense packing volume fraction is also displayed.

corresponding to the amorphous sample is used to separate the contribution of the residual amorphous phase from the contribution of the crystallized one. Similar estimations were performed for other holding times at 410 °C and the resulting measured crystal volume fraction are summarized in Table 1. A continuous increase of $f_v$ with the heating time is obtained up to 60 min where a maximum value of 0.45 is attained.

Large differences are consequently highlighted between DSC and XRD measurements and especially for the maximum volume fraction measured after 60 min of heat treatment at 410 °C that varies between 0.45 and 0.84 depending on the measurement method.

To discriminate between the two methods, numerical simulation is used to compute the maximum volume fraction attainable depending on the crystal morphology and size distribution. The direct quantification of the crystal volume fraction from TEM observations is not straightforward as demonstrated by Wesseling et al. [19] but TEM allows to get quite precisely a size and morphology distribution of crystallites. TEM observations were analyzed for the tested annealing times (10, 20, 30, 45 and 60 min as shown in Fig. 1) at 410 °C. From these observations, it was concluded that the characteristics of the crystal size distributions and morphology remained roughly constant whatever the annealing time. The only significantly varying parameter during the crystallization process is the number of crystals. A quite large fraction of nearly spherical crystals can be observed with an average radius $r_{average}$ of about 15 nm. The crystal size distribution appears relatively narrow, with minimum and maximum radius values typically between 7 and 35 nm as plotted in Fig. 3. These conclusions suggest that the crystallization characteristics in these conditions of heat treatment and for the given BMG correspond to the rapid development of nearly spherical particles dispersed in the residual amorphous matrix. In the studied alloy, the experimental crystal radius distribution deduced from TEM observations can hence be approximated with a normal law according to:

$$P(r) = \frac{1}{\sigma\sqrt{2\pi}} \exp\left(-\frac{(r - r_{average})}{2\sigma^2}\right) \quad (3)$$

where $P(r)$ is the probability to get a particle with a radius $r$ and $\sigma$ is the standard deviation (see Fig. 3). As already mentioned, whatever the applied holding times at 410 °C, similar characteristics of the crystal size distributions can be used: $r_{average} \approx 15$ nm and $\sigma \approx 3.5$ nm.

Interesting information concerning the possibility to disperse a given population of spheres in a medium can be obtained by appropriate numerical simulations. In the present investigation, we use a simulation allowing the prediction of the maximum volume fraction in a given medium of non-intersecting spheres (with a given size distribution). In this software, spheres are dispersed in a cube with a size of about 30 times the average sphere diameter. For a given population of spheres (i.e. with given size distribution and total number of spheres), the software puts randomly all the spheres one by one, starting from the largest ones and forbidding intersections. Indeed, in such a framework, the selection order of the spheres to be put in the cube will affect the predictions. Since the largest crystals are likely to be the first nucleated ones, it was decided in the simulation to follow the distribution by putting the spheres by decreasing sizes. However, one must note that the use of such a procedure to simulate the crystallization process assumes indirectly that the nucleating crystals grow to their final size and then do not grow significantly anymore; hypothesis that seems to be verified by the TEM measurements of the crystallites size displayed in Fig. 3. When a new sphere is placed in the box, the software checks for intersections with pre-existing spheres of which the positions have been stored. If intersections exist, a new position of the same sphere is randomly chosen, until there are no intersections. The total number of attempts to place all the spheres is thus calculated. Finally, the repetition of this method for various total numbers of spheres allows drawing the required number of attempts as a function of the volume fraction of spheres. To reduce border effects, the total volume fraction of spheres is calculated using particles with gravity center inside the box.

Such drawings are shown in Fig. 4 for various sphere distributions. As far as the volume fraction of spheres increases, the required number of attempts to put all the spheres increases very strongly. From this dependency, a maximum volume fraction of non-intersecting spheres in the medium can be estimated. In the case of spheres with a given constant radius, a maximum value of about 0.37 is predicted, in agreement with previously published values [26]. As expected, this value is significantly lower than the

value of 0.64 of the dense random packing volume fraction of spheres with constant diameters [27]. One can note that values greater than 0.64 are only achievable when the sphere have different diameters and a volume fraction of 1 is achievable only for non-spherical crystallites. The maximum volume fraction attainable with the crystallites radius distribution corresponding to Eq. (3) can also be computed. With these parameters, a maximum volume fraction of non-intersecting crystals of about 0.5 is predicted as represented in Fig. 4.

This value is in agreement with the value deduced from XRD measurements while it is significantly smaller than what is predicted by DSC analysis. This discrepancy with the DSC measurements was expected since, as explained above, DSC measurements are subjected to many approximations. A longer heat treatment of 180 min was also performed with no significant evolution of the crystallite volume fraction measured by XRD since a value of 0.5 was also measured. It tends to show that the crystallization process that occurs at this temperature saturates for such a crystal volume fraction in accordance with the numerical simulations. This also seems to confirm the ability to use XRD measurements is a more appropriate way to get the volume fraction of crystals in partially crystallized metallic glasses, at least in the case when volume fraction are not too small since XRD is not appropriate to measure small amount of crystallites. It also suggests that larger crystal volume fractions could be reached only in the case of a wider crystal size distribution (but the resulting effect is expected to be very limited) or with a significant change in the shape of the crystals (as it is obtained when the alloy is heated at higher temperatures [6]).

## 4. Conclusion

The effect of thermal annealing on the Vit1 at 410 °C was analyzed and the crystal volume fraction was measured for various annealing time by XRD and DSC providing significantly different volume fractions of crystallites. The partially crystallized alloy can be described as a dispersion of spherical nanometric particles in an amorphous matrix. By an appropriate numerical simulation, it has been shown that the maximum volume fraction value of crystallites (with a morphology respecting the TEM observations) that can be dispersed in the BMG with no contact between them is 0.5. This value corresponds to the saturated volume fraction measured by XRD and is much smaller than the value measured by DSC. It was concluded that XRD measurements seem to be a more appropriate method to get the crystallite volume fraction in partially crystallized metallic glasses and that care must be taken using DSC measurements.

## References

[1] A. Inoue, Acta Mater. 48 (2000) 279.
[2] K.S. Lee, T.K. Ha, S. Ahn, Y.W. Chang, J. Non Cryst. Solids 317 (2003) 193.
[3] J. Lu, G. Ravichandran, J.L. Johnson, Acta Mater. 51 (2003) 3429–3443.
[4] A.H. Vormelker, O.L. Vatamanu, L. Kecskes, J.J. Lewandowski, Metall. Mater. Trans. A 39A (8) (2008) 1922–1934.
[5] J. Basu, N. Nagendra, Y. Li, U. Ramamurty, Philos. Mag. 83 (2003) 1747.
[6] S. Gravier, A. Mussi, L. Charleux, J.J. Blandin, P. Donnadieu, M. Verdier, J. Alloys Compd. 434–437 (2007) 79–83.
[7] W. Kim, Intermetallics 15 (2007) 282–287.
[8] T.A. Waniuk, R. Busch, A. Masuhr, W.L. Johnson, Acta Mater. 15 (1998) 5229.
[9] W.J. Kim, D.S. Ma, H.G. Jeong, Scripta Mater. 49 (2003) 1067–1073.
[10] M. Bletry, P. Guyot, Y. Brechet, J.J. Blandin, J.L. Soubeyroux, Mater. Sci. Eng. A 387–389 (2004) 1005.
[11] Q. Wang, S. Gravier, J.J. Blandin, J.M. Pelletier, J. Lu, Mater. Sci. Eng. A435–436 (2006) 405.
[12] S. Gravier, Philos. Mag. 88 (2008) 2357–2372.
[13] U. Wolff, N. Pryds, E. Johnson, J.A. Wert, Acta Mater. 52 (2004) 1989.
[14] Z. Bian, G. He, G.L. Chen, Scripta Mater. 46 (2002) 407.
[15] A. Shamimi Nouri, Y. Liu, J.J. Lewandowski, Mater. Trans. A 40A (6) (2009) 1314–1323.
[16] R. Busch, E. Bakke, W.L. Johnson, Acta Mater. 46 (1998) 4725.
[17] C. Fan, D.V. Louzguine, C. Li, A. Inoue, Appl. Phys. Lett. 75 (1999) 340.
[18] K.L. Sahoo, A.K. Panda, S. Das, V. Rao, Mater. Lett. 58 (2004) 316.
[19] P. Wesseling, B.C. Ko, J.J. Lewandowski, Scripta Mater. 48 (2003) 1537.
[20] U. Geyer, S. Schneider, W.L. Johnson, Y. Qiu, T.A. Tombrello, M.P. Macht, Phys. Rev. Lett. 75 (1995) 2364.
[21] J.F. Löffler, W.L. Johnson, Appl. Phys. Lett. 76 (2000) 3394.
[22] A.V. Sergueeva, N. Mara, A.K. Mukherjee, J. Non Cryst. Solids 317 (2003) 169.
[23] A. Guinier, Théorie et technique de la radiocristallographie, Dunod, Paris, 1964, p. 441.
[24] B.E. Warren, X-ray Diffraction, Dover Publications, 1990, p. 122.
[25] Y. He, R.B. Schwarz, D. Mandrus, L. Jacobson, J. Non Cryst. Solids 205–207 (1996) 602.
[26] P. Richard, L. Oger, J.P. Troadec, A. Gervois, Physica A 259 (2000) 205.
[27] S. Torquato, Random Heterogeneous Materials, Interdisciplinary Applied Mathematics, vol. 16, Springer, 2002, p. 701.